



The pH-electrodeposition-dependant of Iron Oxide Toward The Physicochemical Characteristics and Electrochemical Performance in Biorefractory Pollutant Degradation

Widya Ernayati Kosimaningrum^{*1,2}, Heri Heriyanto¹, Meri Yulvianti¹, Alia Badra Pitaloka^{1,3}, Muhammad Raja Najahtama¹, Muhammad Aditya Wibisana¹, Yulis Sutianingsih⁴

¹ Chemical Engineering Department, Faculty of Engineering, Universitas Sultan Ageng Tirtayasa, Cilegon 42435, Banten, Indonesia.

² Center for Local Food Innovation, PUI-PT, Universitas Sultan Ageng Tirtayasa, Serang, Banten, Indonesia.

³ Biomass Valorization Laboratory, Center of Excellence, Faculty of Engineering, Universitas Sultan Ageng Tirtayasa, Cilegon 42435, Banten, Indonesia.

⁴ Magister of Chemical Engineering Department, Faculty of Engineering, Universitas Sultan Ageng Tirtayasa, Cilegon 42435, Banten, Indonesia.

ARTICLE INFO

Article history:

Received August 19, 2022

Received in revised form November 11, 2022

Accepted November 17, 2022

Available online May 02, 2023

Keywords :

Biorefractory Pollutant

Electrochemical Degradation

Electrodeposition

Iron Oxide

Nanoparticles

ABSTRACT

Electrodeposition of the iron oxide (Fe_xO_y) nanoparticles on the graphite felt was prepared from a mixture of iron (II) and iron (III) precursor solution with various pHs (2, 7, and 10) by applying a constant current (galvanostatic) of 0.1 A for 30 minutes. Each resulting sample was coded GF/ Fe_xO_y -2, GF/ Fe_xO_y -7, and GF/ Fe_xO_y -10, respectively. Graphite felt without modification, Raw-GF, was used as control. The mass of iron oxide (Fe_xO_y) deposited ranged from 0.02 to 0.03 grams. The product characterisation using a Scanning Electron Microscope (SEM) showed the distribution of 500 nm particles on the surface of the graphite felt for the GF/ Fe_xO_y -2 sample. In comparison, the distribution of larger particles (1 – 2 μm) was observed in the samples of GF/ Fe_xO_y -7 and GF/ Fe_xO_y -10, respectively. Spectrum resulting from an X-ray Diffraction Spectroscopy (XRD) showed the formation of iron oxides (Fe_xO_y) such as magnetite (Fe_3O_4), haematite (Fe_2O_3), goethite (FeOOH), and lepidocrocite ($\text{FeO}(\text{OH})$). Fourier Transform Infra-Red (FTIR) spectrum also confirmed the presence of Fe_2O_3 in the GF/ Fe_xO_y -2 sample, Fe_3O_4 in the GF/ Fe_xO_y -7 and GF/ Fe_xO_y -10 samples, and FeOOH in all three samples. Applying the iron oxide modified graphite felt in the electro-Fenton approach process without aeration showed that it can degrade bio-refractory pollutants, such as methyl orange. The observed degradations of methyl orange were a decrease in the colour intensity up to 81.37% and a decrease in the COD up to 49.85%.

1. INTRODUCTION

Biorefractory pollutants contain recalcitrant organic compounds that cannot be decomposed through conventional biological processes (Barrera-Díaz, Linares-Hernández, Roa-Morales, Bilyeu, & Balderas-Hernández, 2009; Rajoriya, Carpenter, Saharan, & Pandit, 2016). These compounds contain azo bonds (-N=N-) (Guivarch, Trevin, Lahitte, & Oturan, 2003), which are difficult to digest by

microorganisms. Biorefractory organic pollutants are also toxic and carcinogenic to macro- and micro-organisms (X. Yu, Zhou, Hu, Groenen Serrano, & Yu, 2014). Various industries such as textiles, dyes, pesticides, and pharmaceuticals continuously produce large amounts of organic pollutants (Rajoriya et al., 2016), which simultaneously trigger serious pollution problems in both

*Correspondence author.

E-mail : widya.ernayati@untirta.ac.id (Widya Ernayati Kosimaningrum)

doi : <https://10.21771/jrtppi.2023.v14.no.1.p8-18>

2503-5010/2087-0965© 2021 Jurnal Riset Teknologi Pencegahan Pencemaran Industri-BBSPJPI (JRTTPI-BBSPJPI).

This is an open access article under the CC BY-NC-SA license (<https://creativecommons.org/licenses/by-nc-sa/4.0/>).

Accreditation number : (Ristekdikti) 158/E/KPT/2021

surface water and groundwater (X. Yu et al., 2014). Industrial wastes have passed through the treatment system, but the remnants of biorefractory compounds still potentially endanger the health of ecosystems, animals, and humans, even in tiny amounts (X. Yu et al., 2014). Therefore, the existence of a waste treatment system that effectively degrades biorefractory compounds needs to be developed.

Biorefractory organic waste treatment methods that have been developed include adsorption (Iwuozor, Ighalo, Emenike, Ogunfowora, & Igwegbe, 2021), ozonation (Baig & Liechti, 2001), membranes (W. Liu, Howell, Arnot, & Scott, 2001), electrochemical methods (Ganiyu et al., 2018), and advanced oxidation process (AOP) (Rajoriya et al., 2016). The electrochemical method with the AOP approach, the so-called electro-Fenton, is quite effective in degrading the biorefractory compounds of coloured azo compounds such as methyl orange, methyl red, and azo benzene (Guivarch et al., 2003). The electro-Fenton involves the reduction of oxygen at a cathode to generate hydrogen peroxide (HOOH), which can then be decomposed into hydroxide radicals ($\bullet\text{OH}$) in the presence of a Fenton catalyst (Fe^{2+}) (Le et al., 2019). Hydroxide radicals are powerful oxidising agents for the AOP process, which can even degrade various and persistent organic compounds (Rajoriya et al., 2016).

The electro-Fenton process requires oxygen to generate H_2O_2 , Fenton catalysts, and suitable electrodes that can facilitate the oxygen reduction reaction to H_2O_2 . The oxygen in the water as dissolved oxygen is about 9 mg/L (Tai, Yang, Liu, & Li, 2012). The oxygen is usually supplied by purging oxygen gas or compressed atmospheric air to increase its saturation during the electro-Fenton process (Le et al., 2019). In a conventional electro-Fenton, a Fenton catalyst is added to the solution at a pH of 3 (Le et al., 2015). Carbon-based electrode materials are widely used as electrodes to generate H_2O_2 , namely, graphite felt (Kosimaningrum et al., 2017; Miao, Zhu, Tang, Chen, & Wan, 2014), carbon felt (Huong Le, Bechelany, & Cretin, 2017), and activated carbon fibre (X. Yu et al., 2014). Various modifications of the carbon electrode were also carried out to improve its performance in the electro-Fenton process, one of which is by loading nanoparticles catalyst (Lian, Huang, Liang, Li, & Xi, 2019; K. Liu, Yu, Dong, Wu, & Hoffmann, 2018).

Iron oxide (Fe_xO_y) nanoparticles, such as haematite (Fe_2O_3) and magnetite (Fe_3O_4), are materials commonly applied to water and wastewater treatment (Petrov et al., 2020; Stoia, Păcurariu, Istrate, & Nižňanský, 2015). The iron oxide nanoparticles are potential catalysts in the electro-Fenton process (Ben Hafaiedh, Fourcade, Bellakhal, & Amrane, 2020). The iron oxide nanoparticles can be loaded onto carbon-based cathode materials through various processes such as chemical precipitation (Huiqun, Meifang, & Yaogang, 2006), adsorption (Gupta, Agarwal, & Saleh, 2011), encapsulation (Z. Wu, Li, Webley, & Zhao, 2012), and electrodeposition (M.-S. Wu, Ou, & Lin, 2010). In the electro-Fenton process, the iron oxide can be dissociated into Fe^{2+} and Fe^{3+} ions, which catalyse the breakdown of hydrogen peroxide to form hydroxide radicals in the solution (Ben Hafaiedh et al., 2020).

The electrodeposition method has successfully developed the preparation of iron oxide nanostructure, as reported elsewhere (Aghazadeh & Ganjali, 2018; Martinez et al., 2007; M.-S. Wu et al., 2010). This electrochemical method enables the regulation of the deposited nanomaterial by controlling the composition of precursor solution, pH, deposition mode, salt, and bath type. The electrodeposition method reveals a simple one-step process at room temperature, even without an additional capping agent to fabricate iron oxide nanoparticles. The conventional chemical method involves expensive materials, high temperatures, multi-step processes, and long-time synthesis. Thus, in general, electrochemical synthesis has been taken into account as a preferred method in the development of nanostructure materials due to its many advantages over the standard chemical method (Aghazadeh, 2019).

The advantages of the electrodeposition method are as follows; the mild operating conditions that can be carried out at room temperature and pressure, the use of fewer chemicals both in quantity and type, and fast reaction rates. Therefore, this study aimed to synthesise iron oxide, Fe_xO_y , which was carried out using a simple cathodic electrodeposition method on graphite felt carbon substrate in a mixture of iron(II) and iron(III) precursor solutions with various pHs. The electrodeposition product was then tested for its performance as a cathode in the electrochemical

degradation of methyl orange through the electro-Fenton process. During the electro-Fenton process, neither oxygen gas nor compressed air was bubbled into the synthetic wastewater solution for aeration purposes. The novelty of this research was the study of the effect of precursor solution pH on the characteristics of the as-resulted iron oxide modified graphite felt and its performance in the electrochemical degradation of biorefractory compounds.

2. METHODS

2.1. Materials

The materials used in this study were commercial graphite felt technical grade, ethanol (96%) purchased from Bratachem, iron sulfate heptahydrate, $\text{FeSO}_4 \cdot 7\text{H}_2\text{O}$ (99%), iron nitrate nonahydrate, $\text{Fe}(\text{NO}_3)_3 \cdot 9\text{H}_2\text{O}$ (99%), methyl orange, sodium sulfate anhydrous, and sodium hydroxide were purchased from Merck.

2.2. Graphite felt sample preparation

Graphite felt was the basic carbon material to be modified in this study. The graphite felt was washed with 96% ethanol to remove the contaminants. The graphite felt was cut into pieces, 5×10 cm, soaked in 96% ethanol, and then ultrasonicated for 30 minutes. Next, the graphite felt was separated from the ethanol and washed with distilled water three times. The graphite felt was dried in an oven at 60°C for 24 hours. Furthermore, the cleaned and dried graphite felt was stored in a silica gel container.

2.3. Electrodeposition of iron oxide on graphite felt

Iron oxide was coated on graphite felt using the electrodeposition method developed by Aghazadeh & Ganjali (Aghazadeh & Ganjali, 2018) with several modifications. The electrodeposition was carried out in an electrochemical cell containing 125 mL of a 0.005 M precursor solution in the form of a mixture of Fe (II), from $\text{FeSO}_4 \cdot 7\text{H}_2\text{O}$, and Fe (III), from $\text{Fe}(\text{NO}_3)_3 \cdot 9\text{H}_2\text{O}$ with pH variations of 2, 7, and 10, respectively. The graphite felt as a cathode, and the titanium mesh coated with platinum as an anode were set in the cell at a fixed distance of 3 cm. The electrodeposition was carried out, without stirring, by flowing a constant current of 0.1 A (2.4 mA/cm^2) for 30 minutes at room temperature and pressure. The resulting modified graphite felt was dried in a vacuum oven at 60°C for 24 hours. The mass of graphite felt

before and after electrodeposition was weighed to determine the mass of iron oxide deposited on the graphite felt. The iron oxide modified graphite felts, Fe_xO_y , produced from the precursor solution with variations in pH of 2, 7, and 10, were coded as GF/ Fe_xO_y -2, GF/ Fe_xO_y -7, and GF/ Fe_xO_y -10, respectively. Meanwhile, Raw-GF, graphite felt without modification, was used as the experimental control.

2.4. Physicochemical Analysis

The morphology of the electrosynthesis product samples was scanned with a Jeol JSM-6510 scanning electron microscope (SEM). At the same time, the material structure was analysed using an X-Ray Diffraction Spectrophotometer, XRD, Shimadzu XRD-7000, and a Fourier-Transform Infra-Red, FTIR, Perkin Elmer.

2.5. The electrochemical degradation process of synthetic waste

The resulting iron oxide coated graphite felt sample was used as an electrode in the degradation process of synthetic waste. Each sample was cut to a 0.5×10 cm size with an iron oxide coated area of about $0.5 \times 1 \times 3.5$ cm. This iron oxide modified graphite felt was used as a cathode, and the platinum-coated titanium was used as an anode in the electro-Fenton process. The electro-Fenton was carried out on 125 mL of 0.1 mM methyl orange synthetic waste in 0.05 M sodium sulfate solution for 1 hour with a constant current of 0.2 A and continuous stirring. Before and after the electro-Fenton process, the synthetic waste's colour and Chemical Oxygen Demand (COD) were analysed. The colour of the synthetic waste was determined based on the absorbance value of the methyl orange solution measured using a UV-Visible spectrophotometer at a wavelength of 470 nm. Furthermore, the COD of the synthetic waste was measured using the Standard Method 5220D. The colour and COD removal efficiencies were calculated using equations 1 (Parshetti, Telke, Kalyani, & Govindwar, 2010) and 2 (Yang, Liang, Zhang, & Liang, 2016), respectively.

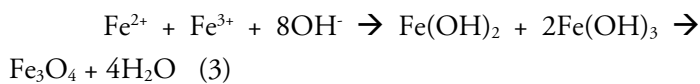
$$\% \text{ colour removal} = \frac{(\text{Initial absorbance} - \text{Final absorbance})}{\text{Initial absorbance}} \times 100\% \quad (1)$$

$$\% \text{ COD removal} = \frac{\text{Initial COD} - \text{final COD}}{\text{Initial COD}} \times 100\% \quad (2)$$

3. RESULT AND DISCUSSION

Figure 1 shows a mixed solution of iron(II) and iron(III), as referred to by Aghazadeh et al. (Aghazadeh &

Ganjali, 2018) at pH of 2, 7, and 10 as a representation of acidic, neutral, and basic conditions. A mixed solution of iron (II) and iron (III) had a pH of 2.36. The solution pH was adjusted to 7 and 10 by adding 5 M NaOH solution dropwise. An increase in pH caused a change in the colour of the solution to dark brown. The solution was brown at a pH of 7 and black at a pH of 10. This indicated that iron(II) and iron(III) ions reacted with hydroxide ions, as stated by Koo et al. in equation 3 (Koo, Ismail, Othman, Rahman, & Sheng, 2019).



The observed colour of the pH-7 solution was brown, resulting from the mixture of the $\text{Fe}(\text{OH})_2$ solution (green) and the $\text{Fe}(\text{OH})_3$ solution (brick red) (Ghernaout et al., 2009). While the colour observed in the pH-10 solution, black, indicated the formation of iron oxide magnetite, Fe_3O_4 (Koo et al., 2019).

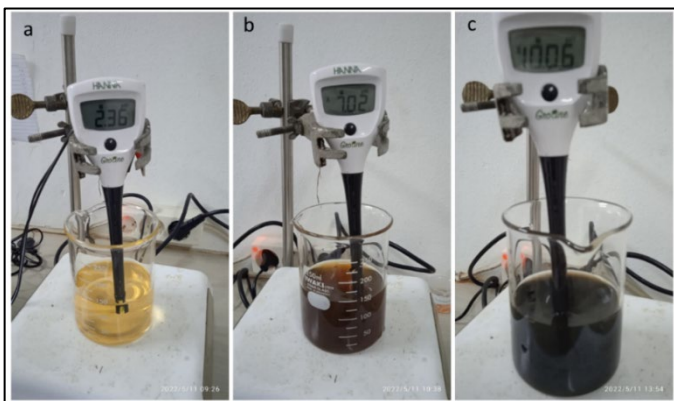


Figure 1. Profile of the mixture of iron (II) and iron (III) precursor solutions at (a) acidic, (b) neutral, and (c) basic pH

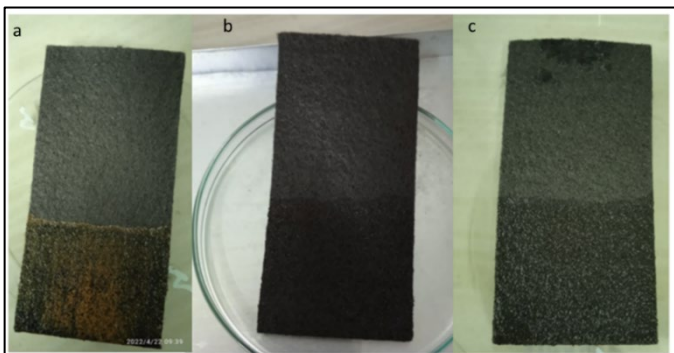


Figure 2. The resulting iron oxide modified graphite felt from the precursor solution at various pH; a. GF/Fe_xO_y -2, b. GF/Fe_xO_y -7, dan c. GF/Fe_xO_y -10

The electrodeposition in each precursor solution was carried out using the galvanostatic method at 2.4 mA/cm² for

30 minutes. Applying the current can cause the oxidation of ferrous ions to ferric oxide. The reaction at the graphite felt cathode was the reduction of water to hydroxide ions and hydrogen gas (equation 4) and the reduction of Fe^{3+} ions to Fe^{2+} ions (equation 5) (Aghazadeh & Ganjali, 2018).



The presence of OH^- ions and Fe^{2+} and Fe^{3+} ions can stimulate the formation of iron oxide magnetite (Fe_3O_4) deposits based on equation 6 on the cathode surface (Aghazadeh & Ganjali, 2018).



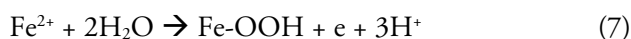
Figure 2 shows the electrodeposition of graphite felt in a solution of iron ion precursors under acidic, neutral, and basic conditions, respectively. On each surface of the graphite felt, the presence of a coating, which was a deposit of iron oxide (Fe_xO_y), can be observed. The deposits formed in the GF/Fe_xO_y -2 sample (Figure 2a) were brown with a mass of 0.02 grams. The brownish iron oxide indicated the iron oxide hematite, Fe_2O_3 . The black deposits in the samples of GF/Fe_xO_y -7 (Figure 2b) and GF/Fe_xO_y-10 (Figure 2c) that weighed 0.03 and 0.02 grams, respectively, indicated the formation of iron oxide magnetite, Fe_3O_4 . Based on the XRD and FTIR spectrum (Fig. 5a and 5b), the GF/Fe_xO_y -7 contains a mixture of haematite and magnetite, which may cause a slightly higher mass than the two other products.

Figure 3 shows the morphology of clean graphite felt (Raw-GF) and the three samples of electrodeposition products, namely GF/Fe_xO_y-2, GF/Fe_xO_y-7, and GF/Fe_xO_y-10 at 1000× magnification. Graphite felt as a support material was composed of carbon fibres with a diameter of about 20 μm. The Raw-GF sample (Figure 3a), which was a sample without modification, showed clean carbon fibres. The GF/Fe_xO_y -2 sample (Figure 3b) showed the distribution of white dots deposited around the carbon fibres. In contrast, the GF/Fe_xO_y -7 (Figure 3c) and GF/Fe_xO_y -10 samples (Figure 3d) showed the presence of deposits on the surface of the carbon fibres in the form of larger particles or lumps.

Figure 4 shows the SEM result of each modified Fe_xO_y electrode with a magnification of 5000× – 10000×. According to Buzea et al., nanoparticles have a size below 1 μm (<1000 nm), while microparticles have a size above 1 μm

(>1000 nm) (Buzea, Pacheco, & Robbie, 2007). Nanoparticle-sized deposits (<500 nm) tended to form in the GF/Fe_xO_y -2 sample (Figures 4a,b), which was produced by electrodeposition in the precursor solution at a pH of 2. Electrodeposition in the precursor solution with pH of 7 produced the deposit of particles, with an approximate size of 500 – 1000 nm (Figures 4c,d), and electrodeposition at pH 10 resulted in the deposit of larger particles size (Figures 4e,f). In an acidic environment, the ions were more dissociated so that the iron ions could quickly spread throughout the surface of the graphite felt. Once the iron ions arrive on the graphite felt surface, they can react with hydroxide ions as a result of water reduction (Aghazadeh & Ganjali, 2018) to form small particles (≤ 500 nm), then were deposited on the surface of the graphite felt. The external addition of hydroxide ions to the solution caused an uncontrolled reaction with iron(II) and iron(III) in the precursor solution. It allowed the formation of larger particles (> 500 nm) which can be deposited as lumps on the graphite felt surface.

Figure 5a shows the spectrum of XRD measurement results. The increase in the pH of the electrodeposition precursor solution increased the intensity in the theta area of 20-30°. Based on the Reference Database Library, the peak at the mentioned area was FeOOH, interpreted as goethite and lepidocrocite, as can be observed in equation 7 (Martinez et al., 2007).



The peak observed in the area between 40 – 50° indicated the existence of iron oxide magnetite, Fe₃O₄. This peak was visible in the electrodeposition sample at a pH of 10. The formation of Fe₃O₄, black deposits on the surface of graphite felt, was effective at a pH above 8. At pH of 7 and 2, magnetite peaks did not appear clearly. Meanwhile, at pH 7 and 2, the 37° area peak was interpreted as forming Fe₂O₃. Furthermore, at a pH of 2, the reddish-brown layer formed was characterised as haematite. The FTIR spectrum of the GF/Fe_xO_y -2 sample (Figure 5b) showed a sharp stretching peak of Fe-O at wave number 594 cm⁻¹ (Fard, Mirjalili, & Najafi, 2018) and 450 cm⁻¹ (Sobhanardakani, Jafari, Zandipak, & Meidanchi, 2018) which were typical for Fe₂O₃. The spectra of GF/Fe_xO_y -7 and GF/Fe_xO_y -10 (Figure 5b) were quite similar to each other, which shows the broad weak

peak in the area between 500 cm⁻¹ and 700 cm⁻¹ as the Fe-O stretching peak of Fe₃O₄ (Raghu et al., 2017).

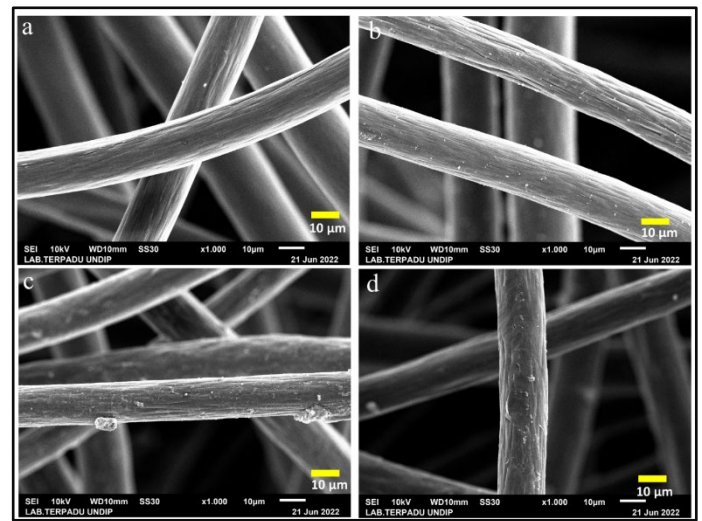


Figure 3. Morphological profile of the sample based on SEM measurements at 1000× magnification for the samples; a) control sample, coded Raw-GF or graphite felt without modification, b. sample GF/Fe_xO_y -2, c. sample GF/Fe_xO_y -7, and d. GF/Fe_xO_y -10.

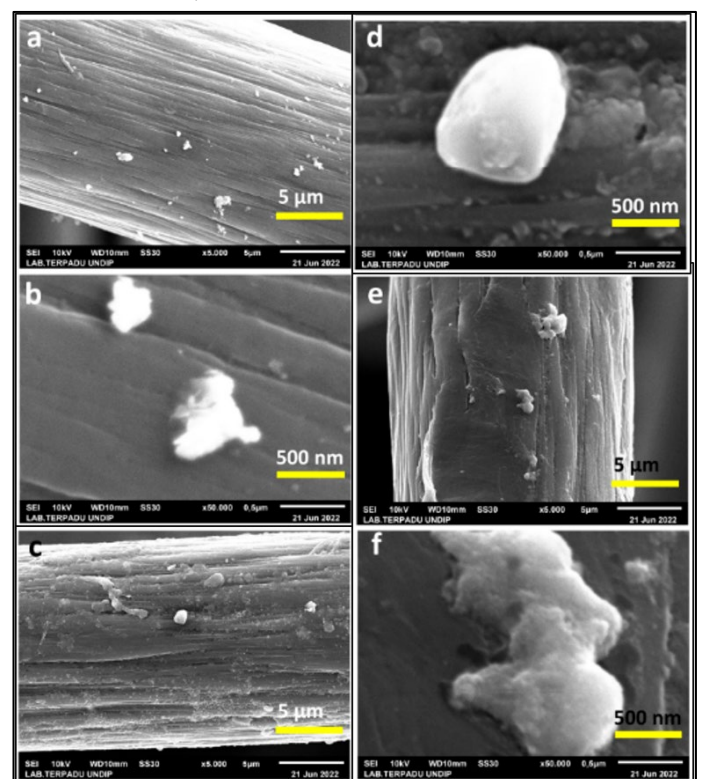


Figure 4 Morphological profile of the samples based on SEM measurements at a magnification of 5000× and 10,000× for the samples; a, b. sample GF/Fe_xO_y -2, c, d. sample GF/Fe_xO_y -7, and e, f. GF/Fe_xO_y -10.

Methyl orange is an organic compound with an azo bond (-N=N-) in its structure, so it is hardly degraded through the conventional microbial degradation method (Han et al., 2015). Furthermore, the ionic sulphonate group makes it very soluble in water (Han et al., 2015), which can quickly spread in aquifers, making it difficult to remove. Therefore, methyl orange can be classified as a biorefractory organic waste that can increase water's chemical oxygen demand (COD) (Guivarch et al., 2003).

In this study, methyl orange was electrochemically degraded using the GF/Fe_xO_y-2, GF/Fe_xO_y-7, and GF/Fe_xO_y-10 samples. Figure 6a shows the methyl orange synthesis waste solution before and after electrochemical treatment. Samples of Raw-GF, GF/Fe_xO_y-2, GF/Fe_xO_y-7, and GF/Fe_xO_y-10 were used as the cathode, and platinum-coated titanium was used as the anode, respectively. Visually, the processed solution showed a significant decrease in colour intensity. Measurements with a UV-Vis spectrophotometer at a wavelength of 470 nm also showed a sharp decrease in absorbance in the post-treatment solution. The average colour loss based on the absorbance measurement results was between 77.69 – 81.43 % for the three modified and the control electrodes (Figure 6b).

The GF/Fe_xO_y-7 resulted in a higher colour removal efficiency than the GF/Fe_xO_y-2. The former contained magnetite (Fe₃O₄), and the latter contained haematite (Fe₂O₃). It showed that Fe₃O₄ had a higher catalytic activity than Fe₂O₃. This result was in line with the study of Prasetyo et al. reporting that Fe₃O₄ was more effective than Fe₂O₃ in the Fenton reaction (Prasetyo, Akbar, Prabandari, & Ariyanto, 2019). However, the GF/Fe_xO_y-10 resulted in a lower colour removal efficiency than the GF/Fe_xO_y-2, although the former dominantly contained Fe₃O₄ and the latter dominantly contained Fe₂O₃. The particle size of the materials caused this. The GF/Fe_xO_y-10 and GF/Fe_xO_y-2 had microparticle and nanoparticle sizes, respectively. The GF/Fe_xO_y-2 was more effective than the GF/Fe_xO_y-10 because the former had a smaller particle size, namely nanoparticle. Graphite felt, a material composed of carbon fibers, can adsorb methyl orange compound in the solution, so the colour of the solution fades. The presence of iron oxide

can aid in colour removal by catalysing the breakdown of azo bonds in methyl orange compounds (Han et al., 2015).

In this study, iron oxide's role was insignificant compared to raw graphite felt (Figure 6b). So, in this case, the colour removal can be inferred to be dominated by the adsorption process. Figure 6b also shows that colour removal was not in line with the COD removal. Concentration, color removal, and COD removal should be in harmony in the case of dilution but not in the case of oxidation. In this research, methyl orange experienced oxidative degradation through a series of breakdowns to form small organic fragments as intermediates and CO₂ and H₂O as the expected final product.

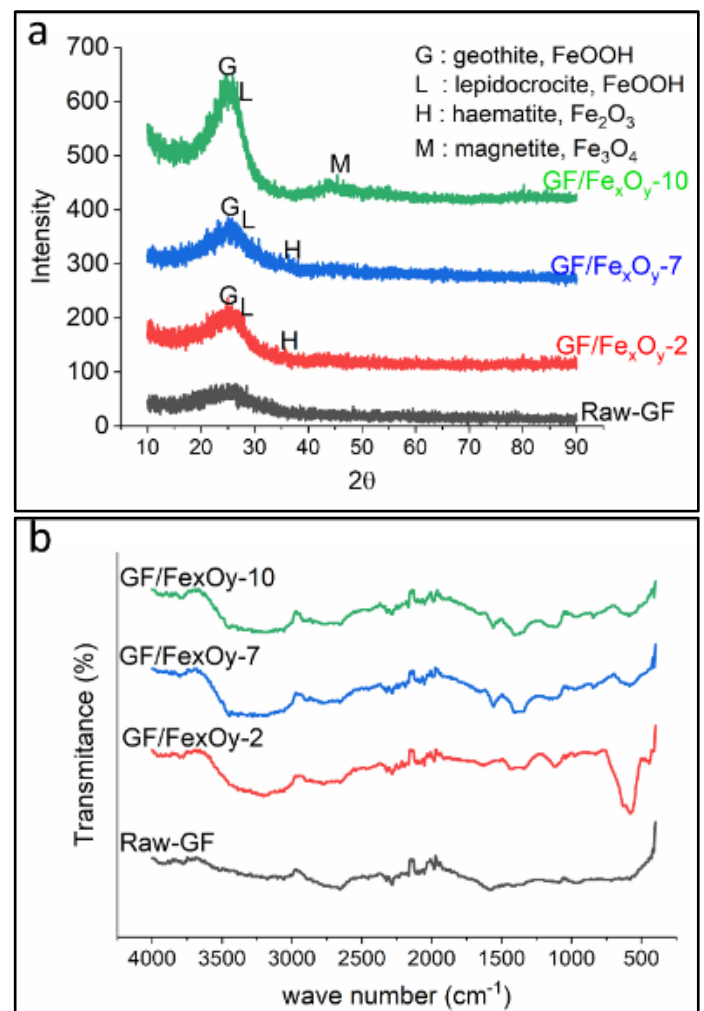
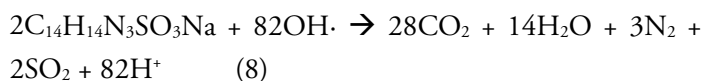


Figure 5. The spectrum of the control and the Fe_xO_y modified graphite felt samples; a. XRD dan b. FTIR

The detailed mechanism of methyl orange degradation has been proposed by Kgatle et al., as shown in Figure 7. Hydroxyl radical attacks the azo bond of the methyl orange, which splits methyl orange into N-N dimethyl-p-phenyl diamine and sulphanic acid. The radical attacks continue the breakdown of these intermediate compounds into many smaller and aliphatic organic fragments. The hydroxyl radicals are expected to oxidize all organic fragments to carbon dioxide completely and water (Kgatle, Sikhwivhilu, Ndlovu, & Moloto, 2021) hence eliminating COD. However, incomplete oxidation can occur, which leaves a high content of small organic fragments and make the COD remain high or increase. In this case, decolourisation can be occurred due to the change of organic compound composition instead of dilution. Initially, methyl orange contains a chromophore group in its structure which is responsible for its colour that absorbs visible light. After the breakdown, the small organic fragments may not contain the chromophore group anymore, and thus, the colour disappears. Herein, the resulting fade colour of the post-oxidation solution may not mean a low COD or organic compound concentration.

The effect of iron oxide was seen in the COD measurement results correlated with the content of organic compounds in the solution (Guivarch et al., 2003). The decrease in COD indicated the presence of mineralization/oxidative degradation of methyl orange with hydroxyl radicals to the inorganic residue, as briefly shown in equation 8. The expected end products are only carbon dioxide and water. However, some other side products, such as SO₂ or acid, considered pollutant compounds, can be emerged. Therefore, other treatments should be conducted before effluent discharge to avoid environmental hazards.



The Raw-GF sample was only able to reduce COD by 20.11 % (Figure 6b), which conforms with the work by Yu et al. (F. Yu, Zhou, & Yu, 2015). The COD removal capability of Raw-GF is predicted due to its adsorptive process. Although Raw-GF also produces hydrogen peroxide (Zhou, Zhou, Hu, Bi, & Serrano, 2014), the formation of hydroxyl radicals for mineralisation is unfeasible due to the

lack of a catalyst. In this research, the addition of iron oxide to graphite felt has affected the methyl orange degradation performance. Iron oxides catalyze the Fenton reaction, which is the breakdown of H₂O₂ to hydroxyl radical and performs oxidative degradation. Herein, The GF/Fe_xO_y-2 sample gave the best COD reduction up to 49.84 %. This result is slightly higher than Santana et al. work which utilized Fe₂O₃/MCM for methyl orange degradation that reached 45 % of COD removal (Sidney Santana, Freire Bonfim, da Cruz, da Silva Batista, & Fabiano, 2021).

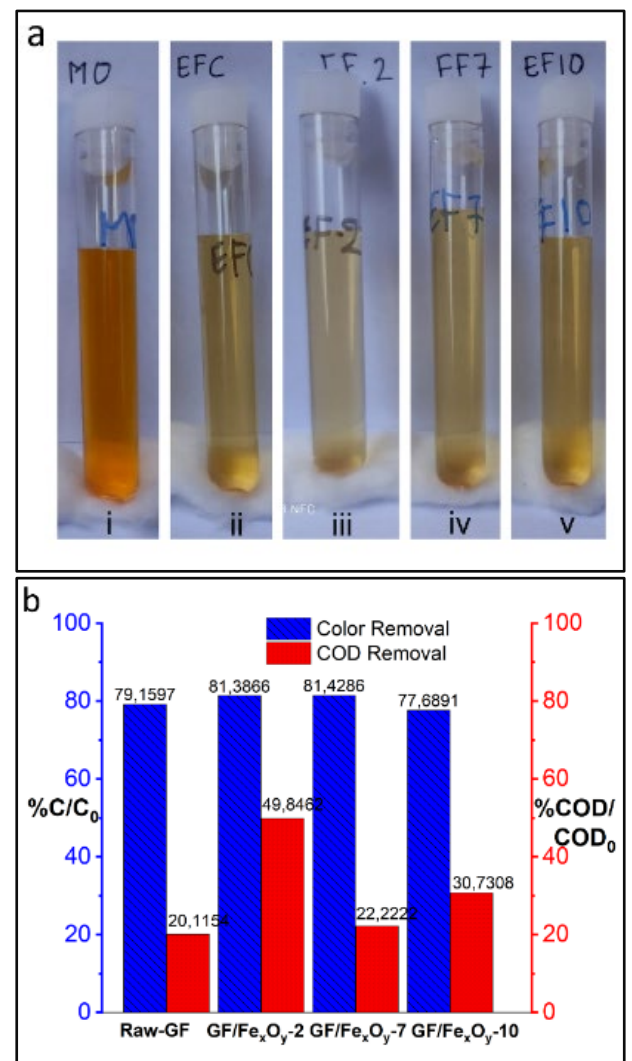


Figure 6. Performance of the iron oxide (Fe_xO_y) modified graphite felt samples upon electrochemical degradation of methyl orange waste; a. the colour of the waste before (i) and after the process (ii – v), b. the colour and COD removal efficiencies

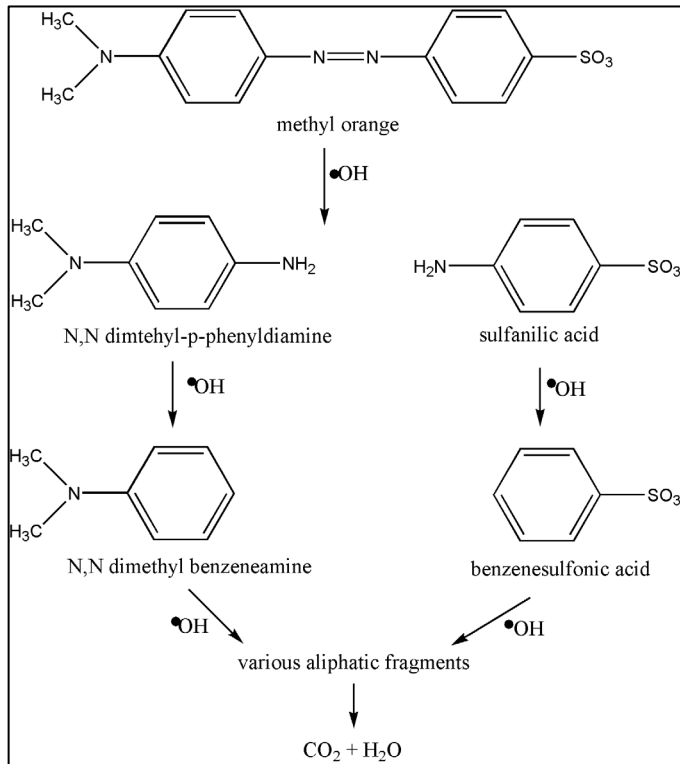


Figure 7 The proposed oxidative methyl orange degradation (Kgatle et al., 2021)

The nanoparticle size of the iron oxide formed on the graphite felt contributes to a better effectivity of the catalyst in the hydroxyl radical generation to conduct mineralisation. The GF/Fe_xO_y-10 sample reduced COD by 30.73%, close to the Jiang et al. work result that used Fe₃O₄ catalyst in methyl orange degradation and reached 32 % of total organic carbon removal (Jiang, Sun, Feng, & Wang, 2016). The GF/Fe_xO_y-10 was indicated to contain iron oxide as magnetite, Fe₃O₄, which has been reported as an effective catalyst in the Fenton reaction (Prasetyo et al., 2019). However, the GF/Fe_xO_y-7 shows only 22.22 % of COD removal. According to its physicochemical characterization, GF/Fe_xO_y-7 contains a mixture of Fe₂O₃ and Fe₃O₄, each having different catalytic properties. The combination of Fe₂O₃ and Fe₃O₄ is predicted to lead to an adverse reaction and incomplete oxidation, leaving abundant small organic fragments and increasing the COD in the post-treatment solution. Thus, the effectiveness of iron oxide on the degradation of methyl orange waste depends on the particle size, the kind, and the composition controlled by the pH (Aghazadeh, 2019) during synthesis.

4. CONCLUSION

The pH of the precursor solution affected the characteristics of the iron oxide (Fe_xO_y) deposited on the graphite felt. In an acid solution (pH of 2), the iron oxide formed indicated the dominant type of FeOOH (goethite and lepidocrocite) and Fe₂O₃ (haematite) as 500 nm. The synthesized iron oxide in neutral (pH of 7) and basic (pH of 10) solutions also indicated the type of FeOOH (goethite and lepidocrocite) and Fe₃O₄ (magnetite) with a particle size of more than 500 nm. The colour removal performances of Raw-GF, GF/Fe_xO_y-2, GF/Fe_xO_y-7, and GF/Fe_xO_y-10 were 79.16 %, 81.39 %, 81.43 %, and 77.69 %, respectively. The GF/Fe_xO_y-2 sample gave a dominant COD reduction of up to 49.84 %, while the GF/Fe_xO_y-7 and the GF/Fe_xO_y-10 sample reduced COD by 22.22 % and 30.73%, respectively. The non-modified graphite felt, Raw-GF, the sample was only able to reduce COD by 20.11 %.

ACKNOWLEDGEMENT

We want to thank the University of Sultan Ageng Tirtayasa, Banten- Indonesia, for the research funding through the 2022 Intermediate Lecturer Research project (PDM 2022).

REFERENCE

- Aghazadeh, M. (2019). Electrochemical Synthesis of Dextran-and Polyethyleneimine-Coated Superparamagnetic Iron Oxide Nanoparticles and Investigation of their Physico-chemical Characters. *ANALYTICAL & BIOANALYTICAL ELECTROCHEMISTRY*, 11(3), 362–372.
- Aghazadeh, M., & Ganjali, M. R. (2018). Samarium-doped Fe₃O₄ nanoparticles with improved magnetic and supercapacitive performance: a novel preparation strategy and characterization. *Journal of Materials Science*, 53(1), 295–308. <https://doi.org/10.1007/s10853-017-1514-7>
- Baig, S., & Liechti, P. A. (2001). Ozone treatment for biorefractory COD removal. *Water Science and Technology*, 43(2), 197–204. <https://doi.org/10.2166/wst.2001.0090>
- Barrera-Díaz, C., Linares-Hernández, I., Roa-Morales, G., Bilyeu, B., & Balderas-Hernández, P. (2009). Removal

- of Biorefractory Compounds in Industrial Wastewater by Chemical and Electrochemical Pretreatments. *Industrial & Engineering Chemistry Research*, 48(3), 1253–1258. <https://doi.org/10.1021/ie800560n>
- Ben Hafaiedh, N., Fourcade, F., Bellakhal, N., & Amrane, A. (2020). Iron oxide nanoparticles as heterogeneous electro-Fenton catalysts for the removal of AR18 azo dye. *Environmental Technology*, 41(16), 2146–2153. <https://doi.org/10.1080/09593330.2018.1557258>
- Buzea, C., Pacheco, I. I., & Robbie, K. (2007). Nanomaterials and nanoparticles: Sources and toxicity. *Biointerphases*, 2(4), MR17–MR71. <https://doi.org/10.1116/1.2815690>
- Fard, G. C., Mirjalili, M., & Najafi, F. (2018). Preparation of nano-cellulose/A-Fe₂O₃ hybrid nanofiber for the cationic dyes removal: Optimization characterization, kinetic, isotherm and error analysis. *Bulgarian Chemical Communications*, 50(August), 251–261.
- Ganiyu, S. O., Huong Le, T. X., Bechelany, M., Oturan, N., Papirio, S., Esposito, G., ... Oturan, M. A. (2018). Electrochemical mineralization of sulfamethoxazole over wide pH range using FeII/FeIII LDH modified carbon felt cathode: Degradation pathway, toxicity and reusability of the modified cathode. *Chemical Engineering Journal*, 350, 844–855. <https://doi.org/https://doi.org/10.1016/j.cej.2018.04.141>
- Ghernaout, D., Ghernaout, B., Boucherit, A., Naceur, M. W., Khelifa, A., & Kellil, A. (2009). Study on mechanism of electrocoagulation with iron electrodes in idealised conditions and electrocoagulation of humic acids solution in batch using aluminium electrodes. *Desalination and Water Treatment*, 8(1–3), 91–99. <https://doi.org/10.5004/dwt.2009.668>
- Guivarch, E., Trevin, S., Lahitte, C., & Oturan, M. A. (2003). Degradation of azo dyes in water by Electro-Fenton process. *Environmental Chemistry Letters*, 1(1), 38–44. <https://doi.org/10.1007/s10311-002-0017-0>
- Gupta, V. K., Agarwal, S., & Saleh, T. A. (2011). Chromium removal by combining the magnetic properties of iron oxide with adsorption properties of carbon nanotubes. *Water Research*, 45(6), 2207–2212. <https://doi.org/https://doi.org/10.1016/j.watres.2011.01.012>
- Han, L., Xue, S., Zhao, S., Yan, J., Qian, L., & Chen, M. (2015). Biochar supported nanoscale iron particles for the efficient removal of methyl orange dye in aqueous solutions. *PLoS ONE*, 10(7). <https://doi.org/10.1371/journal.pone.0132067>
- Huiqun, C., Meifang, Z., & Yaogang, L. (2006). Decoration of carbon nanotubes with iron oxide. *Journal of Solid State Chemistry*, 179(4), 1208–1213. <https://doi.org/https://doi.org/10.1016/j.jssc.2005.12.040>
- Huong Le, T. X., Bechelany, M., & Cretin, M. (2017). Carbon felt based-electrodes for energy and environmental applications: A review. *Carbon*, 122, 564–591. <https://doi.org/https://doi.org/10.1016/j.carbon.2017.06.078>
- Iwuozor, K. O., Ighalo, J. O., Emenike, E. C., Ogunfowora, L. A., & Igwegbe, C. A. (2021). Adsorption of methyl orange: A review on adsorbent performance. *Current Research in Green and Sustainable Chemistry*, 4, 100179. <https://doi.org/https://doi.org/10.1016/j.crgsc.2021.100179>
- Jiang, H., Sun, Y., Feng, J., & Wang, J. (2016). Heterogeneous electro-Fenton oxidation of azo dye methyl orange catalyzed by magnetic Fe₃O₄ nanoparticles. *Water Science and Technology*, 74(5), 1116–1126. <https://doi.org/10.2166/wst.2016.300>
- Kgatle, M., Sikhwivhilu, K., Ndlovu, G., & Moloto, N. (2021). Degradation Kinetics of Methyl Orange Dye in Water Using. *Catalysts*, 11, 428.
- Koo, K. N., Ismail, A. F., Othman, M. H. D., Rahman, M. A., & Sheng, T. Z. (2019). Preparation and characterization of superparamagnetic magnetite (Fe₃O₄) nanoparticles: A short review. *Malaysian Journal of Fundamental and Applied Sciences*, 15(1), 23–31.
- Kosimaningrum, W. E., Le, T. X. H., Holade, Y., Bechelany, M., Tingry, S., Buchari, B., ... Cretin, M. (2017).

- Surfactant- and Binder-Free Hierarchical Platinum Nanoarrays Directly Grown onto a Carbon Felt Electrode for Efficient Electrocatalysis. *ACS Applied Materials & Interfaces*, 9(27), 22476–22489. <https://doi.org/10.1021/acsami.7b04651>
- Le, T. X. H., Bechelany, M., Lacour, S., Oturan, N., Oturan, M. A., & Cretin, M. (2015). High removal efficiency of dye pollutants by electron-Fenton process using a graphene based cathode. *Carbon*, 94, 1003–1011. <https://doi.org/10.1016/j.carbon.2015.07.086>
- Le, T. X. H., Cowan, M. G., Drobek, M., Bechelany, M., Julbe, A., & Cretin, M. (2019). Fe-nanoporous carbon derived from MIL-53(Fe): A heterogeneous catalyst for mineralization of organic pollutants. *Nanomaterials*, 9(4), 1–11. <https://doi.org/10.3390/nano9040641>
- Lian, T., Huang, C., Liang, F., Li, X., & Xi, J. (2019). Simultaneously Providing Iron Source toward Electro-Fenton Process and Enhancing Hydrogen Peroxide Production via a Fe₃O₄ Nanoparticles Embedded Graphite Felt Electrode. *ACS Applied Materials & Interfaces*, 11(49), 45692–45701. <https://doi.org/10.1021/acsami.9b16236>
- Liu, K., Yu, J. C.-C., Dong, H., Wu, J. C. S., & Hoffmann, M. R. (2018). Degradation and Mineralization of Carbamazepine Using an Electro-Fenton Reaction Catalyzed by Magnetite Nanoparticles Fixed on an Electrocatalytic Carbon Fiber Textile Cathode. *Environmental Science & Technology*, 52(21), 12667–12674. <https://doi.org/10.1021/acs.est.8b03916>
- Liu, W., Howell, J. A., Arnot, T. C., & Scott, J. A. (2001). A novel extractive membrane bioreactor for treating biorefractory organic pollutants in the presence of high concentrations of inorganics: application to a synthetic acidic effluent containing high concentrations of chlorophenol and salt. *Journal of Membrane Science*, 181(1), 127–140. [https://doi.org/https://doi.org/10.1016/S0376-7388\(00\)00496-8](https://doi.org/https://doi.org/10.1016/S0376-7388(00)00496-8)
- Martinez, L., Leinen, D., Martín, F., Gabas, M., Ramos-Barrado, J. R., Quagliata, E., & Dalchiale, E. A. (2007). Electrochemical Growth of Diverse Iron Oxide (Fe₃O₄, α-FeOOH, and γ-FeOOH) Thin Films by Electrodeposition Potential Tuning. *Journal of The Electrochemical Society*, 154(3), D126. <https://doi.org/10.1149/1.2424416>
- Miao, J., Zhu, H., Tang, Y., Chen, Y., & Wan, P. (2014). Graphite felt electrochemically modified in H₂SO₄ solution used as a cathode to produce H₂O₂ for pre-oxidation of drinking water. *Chemical Engineering Journal*, 250, 312–318. <https://doi.org/https://doi.org/10.1016/j.cej.2014.03.043>
- Parshetti, G. K., Telke, A. A., Kalyani, D. C., & Govindwar, S. P. (2010). Decolorization and detoxification of sulfonated azo dye methyl orange by *Kocuria rosea* MTCC 1532. *Journal of Hazardous Materials*, 176(1–3), 503–509. <https://doi.org/10.1016/j.jhazmat.2009.11.058>
- Petrov, D. A., Lin, C. R., Ivantsov, R. D., Ovchinnikov, S. G., Zharkov, S. M., Yurkin, G. Y., ... Lyubutin, I. S. (2020). Characterization of the iron oxide phases formed during the synthesis of core-shell Fe_xO_y@C nanoparticles modified with Ag. *Nanotechnology*, 31(39). <https://doi.org/10.1088/1361-6528/ab9af2>
- Prasetyo, I., Akbar, F., Prabandari, A. W., & Ariyanto, T. (2019). Fenton Oxidation using Easily Recoverable Catalyst of Magnetite (Fe₃O₄) as an Efficient Approach to Treatment of Rhodamine B Dyeing Effluent in Traditional Fabrics Industry. *ASEAN Journal on Science and Technology for Development*, 36(3), 103–108. <https://doi.org/10.29037/ajstd.592>
- Raghu, M. S., Yogesh Kumar, K., Prashanth, M. K., Prasanna, B. P., Vinuth, R., & Pradeep Kumar, C. B. (2017). Adsorption and antimicrobial studies of chemically bonded magnetic graphene oxide-Fe₃O₄ nanocomposite for water purification. *Journal of Water Process Engineering*, 17(March), 22–31. <https://doi.org/10.1016/j.jwpe.2017.03.001>
- Rajoriya, S., Carpenter, J., Saharan, V. K., & Pandit, A. B. (2016). Hydrodynamic cavitation: An advanced oxidation process for the degradation of bio-refractory pollutants. *Reviews in Chemical Engineering*, 32(4), 379–411. <https://doi.org/10.1515/revce-2015-0075>

- Sidney Santana, C., Freire Bonfim, D. P., da Cruz, I. H., da Silva Batista, M., & Fabiano, D. P. (2021). Fe₂O₃/MCM-41 as catalysts for methyl orange degradation by Fenton-like reactions. *Environmental Progress & Sustainable Energy*, 40(2), e13507. <https://doi.org/https://doi.org/10.1002/ep.13507>
- Sobhanardakani, S., Jafari, A., Zandipak, R., & Meidanchi, A. (2018). Removal of heavy metal (Hg(II) and Cr(VI)) ions from aqueous solutions using Fe₂O₃@SiO₂ thin films as a novel adsorbent. *Process Safety and Environmental Protection*, 120(October), 348–357. <https://doi.org/10.1016/j.psep.2018.10.002>
- Stoia, M., Păcurariu, C., Istrate, R., & Nižňanský, D. (2015). Solvothermal synthesis of magnetic Fe_xO_y/C nanocomposites used as adsorbents for the removal of methylene blue from wastewater. *Journal of Thermal Analysis and Calorimetry*, 121(3), 989–1001. <https://doi.org/10.1007/s10973-015-4641-x>
- Tai, H., Yang, Y., Liu, S., & Li, D. (2012). A Review of Measurement Methods of Dissolved Oxygen in Water BT - Computer and Computing Technologies in Agriculture V. In D. Li & Y. Chen (Eds.) (pp. 569–576). Berlin, Heidelberg: Springer Berlin Heidelberg.
- Wu, M.-S., Ou, Y.-H., & Lin, Y.-P. (2010). Electrodeposition of iron oxide nanorods on carbon nanofiber scaffolds as an anode material for lithium-ion batteries. *Electrochimica Acta*, 55(9), 3240–3244. <https://doi.org/https://doi.org/10.1016/j.electacta.2009.12.100>
- Wu, Z., Li, W., Webley, P. A., & Zhao, D. (2012). General and controllable synthesis of novel mesoporous magnetic iron oxide@carbon encapsulates for efficient arsenic removal. *Advanced Materials*, 24(4), 485–491. <https://doi.org/10.1002/adma.201103789>
- Yang, H., Liang, J., Zhang, L., & Liang, Z. (2016). Electrochemical oxidation degradation of methyl orange wastewater by Nb/PbO₂ electrode. *International Journal of Electrochemical Science*, 11(2), 1121–1134.
- Yu, F., Zhou, M., & Yu, X. (2015). Cost-effective electro-Fenton using modified graphite felt that dramatically enhanced on H₂O₂ electro-generation without external aeration. *Electrochimica Acta*, 163, 182–189. <https://doi.org/https://doi.org/10.1016/j.electacta.2015.02.166>
- Yu, X., Zhou, M., Hu, Y., Groenen Serrano, K., & Yu, F. (2014). Recent updates on electrochemical degradation of bio-refractory organic pollutants using BDD anode: a mini review. *Environmental Science and Pollution Research*, 21(14), 8417–8431. <https://doi.org/10.1007/s11356-014-2820-0>
- Zhou, L., Zhou, M., Hu, Z., Bi, Z., & Serrano, K. G. (2014). Chemically modified graphite felt as an efficient cathode in electro-Fenton for p-nitrophenol degradation. *Electrochimica Acta*, 140, 376–383. <https://doi.org/10.1016/j.electacta.2014.04.090>